IEEE Access
Multidisciplinary ⋮ Rapid Review ⋮ Open Access Journal

Received October 2, 2020, accepted October 5, 2020, date of publication October 15, 2020, date of current version November 3, 2020.

Digital Object Identifier 10.1109/ACCESS.2020.3031466

User Selection for Millimeter Wave Non-Uniform Full Dimensional MIMO

İREM CUMALI[1], (Graduate Student Member, IEEE), BERNA ÖZBEK[1], (Senior Member, IEEE), RAO MUMTAZ[2], (Senior Member, IEEE), AND JONATHAN GONZALEZ[2], (Senior Member, IEEE)

[1]Electrical and Electronics Engineering Department, Izmir Institute of Technology, 35430 Izmir, Turkey
[2]GS-LDA, 3810-193 Aveiro, Portugal

Corresponding author: Berna Özbek (bernaozbek@iyte.edu.tr)

This work was supported by the European Union Horizon 2020, RISE 2018 Scheme (H2020-MSCA-RISE-2018) through the Marie Skłodowska-Curie Grant 823903 (RECENT).

ABSTRACT The millimeter wave (mmWave) based full-dimensional (FD) MIMO communication is one of the promising technology to fulfill the demand of high data rate for the sixth generation (6G) services including 6D hologram, haptic and multi-sensory communications. In order to satisfy the requirements of 6G applications, we investigate a non-uniform rectangular array (NURA) structure with FD-MIMO antenna systems for the multiuser mmWave communications. For the dense scenarios where the number of users to be served is high, we propose user selection algorithms for both digital and hybrid transceiver designs in FD-MIMO with NURA for the multiuser mmWave communications. For the digital transceivers, the users are selected based on their channel correlation considering FD-MIMO with NURA structures. For the hybrid transceivers, sequential user and beam selection is performed using the correlation between the beamspace channels in FD-MIMO with NURA case. The superiority of the NURA compared to uniform antenna structure is shown through the performance evaluations in the multiuser mmWave communications. Besides, the sum data rate results and complexity analysis denote the feasibility of the proposed algorithms compared to the joint user and beam selection schemes.

INDEX TERMS Full dimensional MIMO, millimeter wave, non-uniform rectangular array, user selection.

I. INTRODUCTION

For the next generation of wireless networks, millimeter wave (mmWave) communication has drawn great interest to respond to the need for ever-increasing data traffic. From indoor hotspots to the Internet of Vehicles, mmWave communication has a wide range of applications in the next generation networks [1]–[3]. On the other hand, full dimensional MIMO (FD-MIMO) provides a practical solution to the space limitation issue in massive MIMO systems. So, mmWave communication can be combined with the concept of FD-MIMO which utilizes uniform rectangular array (URA) instead of uniform linear arrays (ULA). Thus, mmWave based FD-MIMO systems can meet the demands of sixth generation (6G) services such as 6D hologram, haptic and multi-sensory communications.

In fact, FD-MIMO realizes three dimensional (3D) spatial channel based on the Kronecker product and enables 3D beamforming achievable, which corresponds to simultaneous beamforming in azimuth and elevation domains [4], [5]. On the other hand, in the mmWave communication, the FD-MIMO with URA is less spectrum efficient than the MIMO with ULA having the same number of antenna elements due to the low resolution in the elevation domain [6]. In order to enhance the spectral efficiency in FD-MIMO systems, non-uniform rectangular array (NURA) structure which has a non-uniform antenna distribution in the elevation domain has been presented in [7]. Non-uniform spacing which can be greater than half wavelength between the antenna elements reduces the channel correlation in the multiuser systems. Therefore, the performance of the downlink multiuser system can be enhanced by utilizing NURA at the base station (BS). For the mmWave communication systems, the NURA configuration has been examined in [8] by considering only the channel estimation aspects.

For a multiuser system, the BS may not serve a large number of users simultaneously due to the hardware limitations. Thus, the users are selected to be served in the same

The associate editor coordinating the review of this manuscript and approving it for publication was Irfan Ahmed.

frequency-time resource block. In this case, the user selection method in which all the combinations of user subsets are investigated gives the best performance. However, this method involves excessive computational load especially for a large number of users in dense scenarios which could be the most applicable case for 6G systems. In order to avoid such an exhaustive search, in the literature, the suboptimal algorithms have been presented for sub-6 GHz communications systems in [9]. For the downlink mmWave communication, the user selection algorithms, which are based on the channel gains and the angle of departure information of the users, have been presented in [10]. Moreover, [11] has presented a user selection method based on the semi-orthogonality for the uplink multiuser transmission in mmWave wireless LAN (WLAN), and [12] has examined a chordal distance based uplink user selection scheme utilizing only the angle of arrival information when the hybrid beamformer uses low-resolution analog-to-digital converters. On the other hand, [13] and [14] have considered the user selection schemes for downlink mmWave multiuser MIMO systems. However, [13] has employed the phased-zero-forcing hybrid precoder to determine the analog precoding gain whereas [14] has utilized Discrete Fourier Transform (DFT) codebooks for the analog precoder and combiner.

In the literature, only-beam selection algorithms for mmWave communication have also been examined in [15]–[18]. The authors of [15] have represented the maximum magnitude (MM) beam selection method. In the simplest manner, the MM method allocates a beam whose magnitude is greater than the magnitudes of other possible beams for a user. Although the MM method offers a low complexity beam selection, it neglects the multiuser interference that considerably restricts the system performance. In the mmWave propagation, the channel will be highly correlated when the users are nearly located. Therefore, the MM method assigns the same beam for the users whose channels are highly correlated. Also, assigning the same beam results in a misuse of RF chains, which is impractical. On the other hand, [16]–[18] have represented more complicated beam selection algorithms to address the multiuser interference problem in the MM method. The authors of [16] have introduced multiple algorithms based on the maximization of the signal-to-interference-plus-noise-ratio (SINR) and the capacity. In addition, *Gao et al.* have represented the interference aware (IA) beam selection in [17]. In two stages, the IA method classifies the users by considering the multiuser interferences and selects the beams based on the maximization of the sum data rate. Eventually, two algorithms have been presented in [18] as the heuristic greedy beam selection and the Kuhn-Munkres algorithm based beam selection. In this work, we propose a greedy based approach for the beam selection by considering the multiuser interference problem. So, the proposed beam selection classifies the users as the interfering users and the non-interfering users at each iteration. Then, the algorithm greedily selects the beams.

Furthermore, user selection issue in the mmWave hybrid transceiver has been considered as a joint user and beam selection problem in [19]–[23]. It has been formulated as a non-convex combinatorial optimization problem in [19]–[21] for fully connected hybrid beamforming architecture at the BS. Fully connected architecture connects each RF chain to the antenna array via analog phase shifters. On the other hand, *Jiang et al.* [22] have formulated the problem based on the Lyapunov-drift optimization for beam-based massive MIMO downlinks utilizing the lens array. Also, the problem has been recently solved in [23] through the suboptimal algorithms for the lens array assisted hybrid beamforming architecture. Lens array transforms the spatial domain into the beamspace domain and exploits the sparse structure of the channel. Therefore, there is no need to use phase shifters to concentrate the beams on the desired directions. Since this is advantageous in terms of the hardware cost, in this work, we utilize beam-based or beamspace massive MIMO architecture for the hybrid transceiver. For the user selection issue, the implementation of joint user and beam selection algorithms in the mentioned references becomes more complex, particularly for the massive number of users and antennas. In order to reduce the computational complexity, the user and beam selection can be applied sequentially instead of performing them jointly. Since the selection of users and beams are strongly related to the channel sparsity, we select the users considering their channel characteristics and then we choose the proper beams. Since the mmWave propagation is dominated by the line of sight (LoS) component [24], the highly correlated users usually select the same beam as the strongest one in the beamspace. Hence, we eliminate the highly correlated users to complete the beam selection in few iterations.

Against the above background, our contributions are summarized as follows.

- In this article, we investigate the NURA technology by considering user selection algorithms for mmWave communication with both digital and hybrid transceivers. To the best of the authors' knowledge, this is the first work of its kind in the area of mmWave FD-MIMO using NURA.
- We adopt the exponent-based method [6] to specify the spacing between the adjacent antenna elements in the downlink mmWave communication system. Through the simulations, we figure out the optimal exponent to achieve the optimal structured NURA design based on the sum data rate performance.
- For the digital transceiver in the dense environments, we propose a decremental user selection algorithm based on the correlation through an iterative elimination process. We also demonstrate that the proposed algorithm improves the sum data rate performance by eliminating highly correlated users in the FD-MIMO with NURA design.
- For the hybrid transceiver, we further study the beamspace MIMO concept for the NURA configuration.

Apart from the existing studies in the literature, we propose a sequential user and beam selection algorithm based on the channel norm and the correlation. We indicate that the sum data rate performance of the proposed algorithm approaches the performance of the joint beam and user selection (JBUS) algorithm in [23] while providing substantially lower computational complexity.

The performance results are provided in the mmWave FD-MIMO for URA and NURA structures in both digital and hybrid transceivers. We believe that our work will act as a stepping stone for the upcoming research in the area of the user selection for NURA technology.

Notation: Matrices and vectors are denoted by upper-case and lower-case boldface letters, respectively. $(.)^{-1}$, $(.)^{T}$, $(.)^{H}$, $\|.\|$, $|.|$, $tr(.)$, and $\mathbb{E}\{.\}$ represent the inversion, transpose, conjugate transpose, vector norm, absolute value, trace, and expectation operations, respectively. $Card(.)$ denotes the cardinality of a set, $\cup$ and $\setminus$ represent the union and difference operations for sets, respectively. The field of complex numbers is notated by $\mathbb{C}$ and $\mathbf{0}_n$ is an $n \times n$ dimensional zero matrix. In addition, $\mathbb{C}\mathcal{N}(0, \sigma^2)$ denotes the complex Gaussian random variable with zero mean and variance σ^2, and $\mathcal{U}(a, b)$ denotes the discrete uniform distribution on the interval $[a, b]$. On the other hand, $\mathcal{O}(.)$ is the big-O notation for the complexity analysis.

II. SYSTEM MODEL

In this article, a downlink mmWave communication system based on FD-MIMO with K single-antenna users is considered while K_u users are selected to establish transmission. The BS is equipped with $N_e \times N_a$ dimensional rectangular array having N_e antenna elements in elevation and N_a antenna elements in azimuth domains, and $N_{\text{RF}} \geq K_u$ radio frequency (RF) chains. For the sake of simplicity, it is assumed that the channel state information is perfectly available for all users at the BS.

A. CHANNEL MODEL

The 3D spatial channel defined in [7] has been described for a multipath channel. However, the LoS component of the propagation, which prevails against the multipath components in mmWave communication, is not taken into account in that model. Assuming that the LoS path exists for all users, the channel matrix of k^{th} user can be given by

$$\mathbf{H}_k = \beta_k^{(0)} \mathbf{e}_k^{(0)} \otimes \mathbf{a}_k^{(0)} + \sum_{p=1}^{N_p} \beta_k^{(p)} \mathbf{e}_k^{(p)} \otimes \mathbf{a}_k^{(p)}, \tag{1}$$

where N_p is the number of paths, $\beta_k^{(0)}$ and $\beta_k^{(p)}$ are complex channel gains of the LoS path and the p^{th} path, respectively. The channel matrix $\mathbf{H}_k \in \mathbb{C}^{N_e \times N_a}$ is related with the Kronecker product of the array steering vectors of the elevation $\mathbf{e}_k^{(0)} \in \mathbb{C}^{N_e \times 1}$ and the azimuth $\mathbf{a}_k^{(0)} \in \mathbb{C}^{1 \times N_a}$ for the LoS path, and the array steering vectors of the elevation $\mathbf{e}_k^{(p)} \in \mathbb{C}^{N_e \times 1}$ and the azimuth $\mathbf{a}_k^{(p)} \in \mathbb{C}^{1 \times N_a}$ for the p^{th} path. For describing the steering vectors, a function which expresses the position of each element in the array is required. For the elevation domain, the methods such as exponent-based, exponential, and tangent-based, which define the inter-element spacing, are given in [6]. Furthermore, the authors in [6] has shown that the exponent-based method provides the highest average spectral efficiency for the static array configuration. Therefore, we use the exponent-based method that describes the function $g_\eta(m)$, depending on m, as below

$$g_\eta(m) = d_e\big(N_e - 1\big)\left(\frac{m}{N_e - 1}\right)^{\eta}, \tag{2}$$

where $m = 0, \ldots, N_e - 1$ and $d_e = \lambda/2$. This function can offer a non-uniform antenna distribution in the elevation domain. However, the function $g_{\eta=1}(m) = m d_e$ shows a linear characteristic just like in the azimuth domain. Thus, the array will be URA for the case that provides $\eta = 1$. The exponent value of η can substantially affect the performance of the system. Therefore, we investigate the predetermined exponent value that gives the maximum sum data rate to reach the optimal structured NURA design.

In the azimuth domain, the spacing between adjacent antenna elements is determined by $d_a = \lambda/2$. Therefore, the position of the elements are predefined and the steering vector in the azimuth domain can be expressed by

$$\mathbf{a}_k^{(p)} = \frac{1}{\sqrt{N_a}}\left[1, e^{-j2\pi \frac{d_a}{\lambda}\theta_k^{(p)}}, \ldots, e^{-j2\pi \frac{(N_a-1)d_a}{\lambda}\theta_k^{(p)}}\right], \tag{3}$$

where $\theta_k^{(p)} = sin\vartheta_k^{(p)} cos\varphi_k^{(p)}$ depends on the azimuth angle of departure (A-AoD) $\vartheta_k^{(p)}$ and the elevation angle of departure (E-AoD) $\varphi_k^{(p)}$ for the p^{th} path [4], [25]. The steering vector in the azimuth domain for the LoS path is computed using A-AoD $\vartheta_k^{(0)}$ and E-AoD $\varphi_k^{(0)}$ in (3). By using the positioning function, the array steering vector in the elevation domain is described by

$$\mathbf{e}_k^{(p)} = \frac{1}{\sqrt{N_e}}\left[1, e^{-j2\pi \frac{g(1)}{\lambda}\phi_k^{(p)}}, \ldots, e^{-j2\pi \frac{g(N_e-1)}{\lambda}\phi_k^{(p)}}\right]^T, \tag{4}$$

where $\phi_k^{(p)} = sin\varphi_k^{(p)}$ [6]. However, because of the small angular spread in the elevation domain, all the paths can be approached to a single path such that $\mathbf{e}_k^{(p)} \approx \mathbf{e}_k$, $\forall p$. Therefore, the channel defined in (1) can be degraded to [7]

$$\mathbf{H}_k \approx \beta_k^{(0)} \mathbf{e}_k^{(0)} \otimes \mathbf{a}_k^{(0)} + \mathbf{e}_k \otimes \sum_{p=1}^{N_p} \beta_k^{(p)} \mathbf{a}_k^{(p)}. \tag{5}$$

B. DIGITAL TRANSCEIVER

In the digital transceiver illustrated in Fig. 1, each antenna in the transmitter is connected to a separate RF chain to transmit the parallel data streams.

For the k^{th} user, the received signal can be given as

$$r_k = \mathbf{h}_k^H \mathbf{x} + n_k, \tag{6}$$

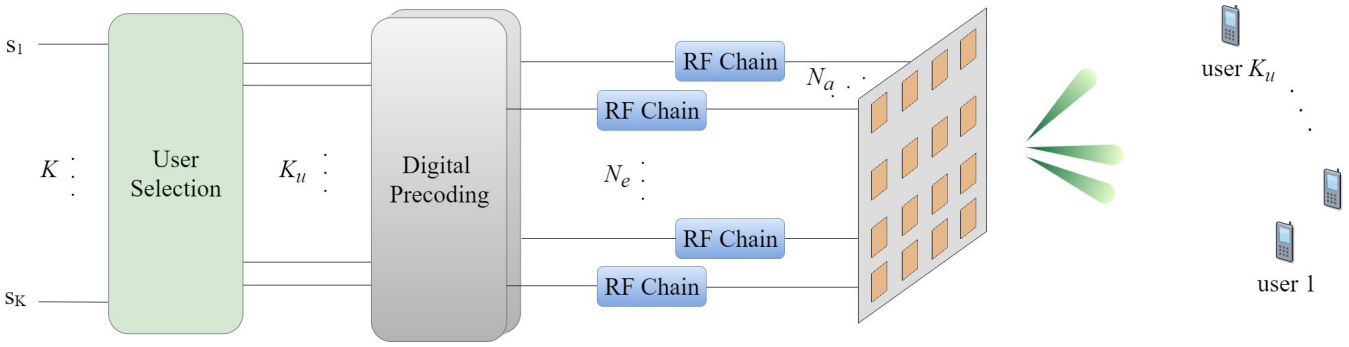

FIGURE 1. System model of the FD-MIMO for the digital transceiver with NURA.

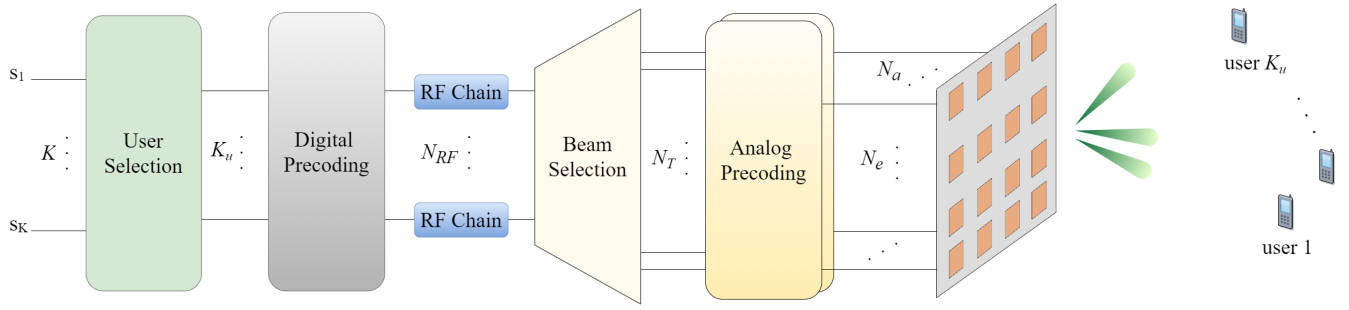

FIGURE 2. System model of the FD-MIMO for the hybrid transceiver with NURA.

where $\mathbf{h}_k \in \mathbb{C}^{N_e N_a \times 1}$ is a vector form of the channel matrix $\mathbf{H}_k$, namely $\mathbf{h}_k = vec(\mathbf{H}_k)$, $\mathbf{x} \in \mathbb{C}^{N_e N_a \times 1}$ denotes the vector of transmitted symbols and n_k is the additive white Gaussian noise (AWGN) modelled by $\mathbb{CN}(0, \sigma^2)$ at the k^{th} user. Thus, the whole system equation can be written as

$$\mathbf{r} = \mathbf{HWs} + \mathbf{n}, \tag{7}$$

where $\mathbf{H} = [\mathbf{h}_1, \mathbf{h}_2, \ldots, \mathbf{h}_{K_u}]^T \in \mathbb{C}^{K_u \times N_e N_a}$, the corresponding precoding matrix is denoted by $\mathbf{W} \in \mathbb{C}^{N_e N_a \times K_u}$, $\mathbf{s} = [s_1, s_2, \ldots, s_{K_u}]^T$ is the symbol vector for K_u users and $\mathbf{n}$ represents the AWGN vector. For the precoding scheme, $\mathbf{W}$ can be computed directly over $\mathbf{H}$ or by vectorizing $\mathbf{H}$ such that $\acute{\mathbf{h}} = vec(\mathbf{H})$ where $\acute{\mathbf{h}} \in \mathbb{C}^{1 \times K_u N_e N_a}$. The zero forcing (ZF) precoder matrix is determined by

$$\mathbf{W} = \alpha \mathbf{H}^H \left(\mathbf{HH}^H\right)^{-1}, \tag{8}$$

where $\mathbf{W} = [\mathbf{w}_1, \mathbf{w}_2, \ldots, \mathbf{w}_{K_u}]$ and the scaling factor can be written as

$$\alpha = \sqrt{\frac{1}{tr\left(\left(\mathbf{HH}^H\right)^{-1}\right)}}. \tag{9}$$

Then, the sum data rate is calculated by

$$R = \sum_{k=1}^{K_u} \mathbb{E}\left\{ \log_2 \left(1 + \frac{\left|\mathbf{h}_k^H \mathbf{w}_k\right|^2}{\sum_{i=1; i \neq k}^{K_u} \left|\mathbf{h}_k^H \mathbf{w}_i\right|^2 + 1/\rho}\right)\right\}, \tag{10}$$

where ρ is the average signal-to-noise ratio (SNR) and the total transmit power is equally shared among K_u users.

C. HYBRID TRANSCEIVER

In the system utilizing a hybrid beamforming transceiver shown in Fig. 2, each antenna element is not connected to a separate RF chain since the number of RF chains is less than the number of transmit antennas. The transmitter employs both digital and analog precoders that results in the hybrid beamforming. By the analog precoder, the antenna or spatial domain is transformed into the beamspace domain [26].

1) BEAMSPACE CHANNEL

Millimeter wave introduces a quasi-optical propagation by its nature. Therefore, the scattering capability of the propagation is limited, providing a dominant LoS component. Accordingly, the mmWave channel exhibits a sparse structure that makes the transformation into the beamspace domain inevitable. The beamspace channel is the virtual representation of the spatial MIMO channel, and the transformation is realized by the analog beamforming matrix of $\mathbf{U}$. For the rectangular array, the beamforming matrix is defined as $\mathbf{U} = \mathbf{U_e} \otimes \mathbf{U_a}$ [27] such that

$$\mathbf{U_e} = \frac{1}{\sqrt{N_e}}\left[1, e^{-j2\pi\phi_n}, \ldots, e^{-j2\pi\phi_n(N_e-1)}\right] \in \mathbb{C}^{N_e \times N_e},$$
$$\mathbf{U_a} = \frac{1}{\sqrt{N_a}}\left[1, e^{-j2\pi\theta_n}, \ldots, e^{-j2\pi\theta_n(N_a-1)}\right] \in \mathbb{C}^{N_a \times N_a}. \tag{11}$$

The specified directions $\phi_n = i_e/N_e$ and $\theta_n = i_a/N_a$ are generated by dividing the elevation space into N_e and the azimuth space into N_a where $i_e \in \{0, \ldots, N_e - 1\}$ and

$i_a \in \{0, \ldots, N_a - 1\}$. The beamforming matrix $\mathbf{U} \in \mathbb{C}^{N_e N_a \times N_e N_a}$ is a unitary DFT matrix such that $\mathbf{U}\mathbf{U}^H = \mathbf{U}^H\mathbf{U} = \mathbf{I}$, and it provides $N_\mathrm{T} = N_e \times N_a$ orthogonal beams. When the channel matrix that includes the channel coefficients of all K users is described by $\bar{\mathbf{H}} \in \mathbb{C}^{K \times N_e N_a}$, the beamspace channel matrix $\bar{\mathbf{H}}_b$ can be written via the beamforming matrix as follows

$$\bar{\mathbf{H}}_b = \bar{\mathbf{H}}\mathbf{U}, \tag{12}$$

where $\bar{\mathbf{H}}_b = [\bar{\mathbf{h}}_{b,1}, \bar{\mathbf{h}}_{b,2}, \ldots, \bar{\mathbf{h}}_{b,K}]^T \in \mathbb{C}^{K \times N_e N_a}$. $\bar{\mathbf{H}}_b$ also includes the channels of all K users in the beamspace domain.

It may be remarked that the beamspace channel has only a few non-zero coefficients. Therefore, the sparse nature of the beamspace channel makes the beam selection feasible without a significant performance loss. In this way, the dimension of the system can be degraded so that the hardware complexity and the power consumption of the system can be reduced.

III. PROPOSED USER SELECTION ALGORITHMS

In this section, the proposed selection algorithms for both the digital and the hybrid transceivers are described. For the digital transceiver, the proposed algorithm utilizes the correlation information between the users' channels to maximize the sum data rate. The non-uniform spacing of the NURA structure can reduce the channel correlation between the users since the spacing between two antenna elements in the array can be greater than the half wavelength [8]. However, it could not still be zero in the NURA for dense scenarios. Therefore, our purpose is to select users whose channels are as much as orthogonal. On the other hand, hybrid transceiver applies the beamspace transformation to exploit the low dimensional system. The proposed algorithm utilizes the channel norm primarily and then the channel correlation between the users to select the beams iteratively in the beamspace domain.

A. USER SELECTION FOR DIGITAL TRANSCEIVER

In the digital system, the number of antennas and RF chains is $N_\mathrm{RF} = N_\mathrm{T}$ where $N_\mathrm{T} = N_e \times N_a$. On the other hand, the system has a higher number of users than the RF chains, $K > N_\mathrm{RF}$ in the dense environment. However, the number of users that can be served by the system is N_RF at most, and $K_u \leq N_\mathrm{RF}$ users must be selected while maximizing the sum data rate. A decremental user selection algorithm is proposed so that K_u users can be served among K users.

Firstly, we determine the correlation between all K users. Based on the correlation values, the proposed algorithm eliminates $(K - K_u)$ users in $(K - K_u)$ iterations. The rows of the spatial channel matrix $\bar{\mathbf{H}} = [\bar{\mathbf{h}}_1, \bar{\mathbf{h}}_2, \ldots, \bar{\mathbf{h}}_K]^T$ correspond to the channel vectors of the users. Therefore, the correlation between i^{th} and j^{th} users is described by

$$\mathrm{c}(i,j) = \frac{|\bar{\mathbf{H}}(i,:)\bar{\mathbf{H}}(j,:)^H|}{\|\bar{\mathbf{H}}(i,:)\|\|\bar{\mathbf{H}}(j,:)\|}. \tag{13}$$

At each iteration, the proposed algorithm calculates the correlation matrix $\mathbf{C}$ whose $(i,j)^{th}$ element $\mathbf{C}_{i,j}$ is equal to $\mathrm{c}(i,j)$. Then, the user pair $\kappa = (\kappa_1, \kappa_2)$ that has the maximum correlation value is determined over $\mathbf{C}$. In this pair, the user that has the lowest channel gain is eliminated to maximize the sum data rate. Finally, the resulting matrix $\hat{\mathbf{H}}$ that has a lower dimension is constituted by ejecting the channel vector of that user from the channel matrix. The proposed algorithm is described in Algorithm 1. The number of rows n_r, which is initially equal to K, is redetermined at each iteration, and the proposed algorithm continues to eliminate a user until there are K_u users left, meaning that n_r in the last iteration is equal to K_u. The resulting channel matrix can be determined as

$$\hat{\mathbf{H}} = \left[\bar{\mathbf{H}}(s,:)\right]_{s \in \mathcal{U}}, \tag{14}$$

where $\mathcal{U}$ is the set of remaining users after the elimination, and $Card(\mathcal{U}) = K_u$.

Algorithm 1 Proposed User Selection Algorithm for Digital Transceiver

Input: $\bar{\mathbf{H}} \in \mathbb{C}^{K \times N_\mathrm{T}}$ in
Output: $\hat{\mathbf{H}} \in \mathbb{C}^{K_u \times N_\mathrm{T}}$ out

```
Initialize Ĥ = H̄, n_r = K
while n_r > K_u do
    Set C = 0_{n_r}
    for i = 1 → n_r do
        for j = i + 1 → n_r do
            C_{i,j} = c(i, j)
        end for
    end for
    Find (κ1, κ2) such that C_{κ1,κ2} = max(C)
    if ||Ĥ(κ1, :)|| ≤ ||Ĥ(κ2, :)|| then
        Eliminate the κ1^th user channel from Ĥ
    else
        Eliminate the κ2^th user channel from Ĥ
    end if
    [n_r, n_c] = size(Ĥ)
end while
```

After the selection of K_u users is completed through **Algorithm 1**, the ZF precoding is performed as given in (8) using the $K_u \times N_\mathrm{T}$ dimensional resulting channel matrix of $\hat{\mathbf{H}}$.

B. USER SELECTION FOR HYBRID TRANSCEIVER

In the hybrid FD-MIMO system, the number of transmit antennas is higher than the number of RF chains, and the number of users is higher than the number of RF chains in a dense environment as $N_\mathrm{T} > K > N_\mathrm{RF}$. Therefore, the beams need to be allocated to the selected users. The proposed user and beam selection algorithm is described in Algorithm 2 in detail. The algorithm includes two steps sequentially as the user selection and the beam selection.

In the first part of the proposed algorithm, the channel norm and the correlation information are utilized to choose the users to be served. As a result, K_u users are selected through the beamspace channel where $K_u = N_\mathrm{RF}$ for the proposed algorithm. At first, the algorithm computes the beamspace channel norm for each user, and the user indices are sorted

Algorithm 2 Proposed User and Beam Selection Algorithm for Hybrid Transceiver

Input: $\bar{\mathbf{H}}_b \in \mathbb{C}^{K \times N_\mathrm{T}}$ in
Output: $\tilde{\mathbf{H}}_b \in \mathbb{C}^{K_u \times K_u}$ out

Part 1: User selection

Determine the channel norms $\mathbf{b}(k) = \left\|\bar{\mathbf{H}}_b(k,:)\right\|, \forall k$
Sort users from highest to lowest by $\mathbf{b}(k)$
Save the user indices to $\mathbf{v}$ in order
Set $\mathcal{U} \leftarrow \mathcal{U} \cup \{\mathbf{v}(1)\}$
Set $n_r = 1$ and $n_i = 2$
while $n_r < K_u$ **do**
  Set $\mathcal{U} \leftarrow \mathcal{U} \cup \{\mathbf{v}(n_i)\}$ and compute $n_r = Card(\mathcal{U})$
  Constitute $\hat{\mathbf{H}}_b = \left[\bar{\mathbf{H}}_b(s,:)\right]_{s\in\mathcal{U}}$
  Set $\mathbf{C}_b = \mathbf{0}_{n_r}$
  for $i = 1 \rightarrow n_r$ **do**
    for $j = i+1 \rightarrow n_r$ **do**
      $\mathbf{C}_{b_{i,j}} = \mathrm{c}_b(i,j)$
    end for
  end for
  if $\max(\mathbf{C}_b) > \epsilon$ **then**
    $\mathcal{U} \leftarrow \mathcal{U} \setminus \{\mathbf{v}(n_i)\}$ and constitute $\hat{\mathbf{H}}_b$ again
  end if
  $n_i \leftarrow n_i + 1$
  Compute n_r again
end while

Part 2: Beam selection

Initialize $\mathcal{K}_r = \{1, \ldots, K_u\}$ and $\mathcal{K}_s = \emptyset$
Initialize $\mathcal{N}_r = \{1, \ldots, N_\mathrm{T}\}$ and $\mathcal{N}_s = \emptyset$
Initialize $\mathbf{T} = \hat{\mathbf{H}}_b \in \mathbb{C}^{K_u \times N_\mathrm{T}}$
while $Card(\mathcal{K}_r) \neq 0$ **do**
  Set $\mathbf{M}(k,n) = |\mathbf{T}(k,n)|^2, \ \forall k, \forall n.$
  for $k = 1 \rightarrow Card(\mathcal{K}_r)$ **do**
    $\xi_k = \arg\max_{n\in\{1,\ldots,Card(\mathcal{N}_r)\}} \mathbf{M}(k,n)$
  end for
  for $k = 1 \rightarrow Card(\mathcal{K}_r)$ **do**
    if $\xi_k \neq \xi_p$ **then**
      Assign beam ξ_k to user k
      Set $\mathcal{K}_\mathrm{NIU} \leftarrow \mathcal{K}_\mathrm{NIU} \cup \{k\}$, $\mathcal{N}_\mathrm{NIU} \leftarrow \mathcal{N}_\mathrm{NIU} \cup \{\xi_k\}$
    else
      Set $\mathcal{K}_\mathrm{IU} \leftarrow \mathcal{K}_\mathrm{IU} \cup \{k\}$
    end if
  end for
  Find the subsets $\mathcal{A}_{\xi_m}^{(l)}$ of the set $\mathcal{K}_\mathrm{IU}$
  for $l = 1 \rightarrow L$ **do**
    Assign beam ξ_m to $i = \arg\max_{j\in\mathcal{A}_{\xi_m}^{(l)}} \mathbf{M}(j,\xi_m)$
    Set $\mathcal{K}_{\mathrm{IU}_1} \leftarrow \mathcal{K}_{\mathrm{IU}_1} \cup \{i\}$ and $\mathcal{N}_{\mathrm{IU}_1} \leftarrow \mathcal{N}_{\mathrm{IU}_1} \cup \{\xi_m\}$
  end for
  Set $\mathcal{K}_s \leftarrow \mathcal{K}_s \cup \mathcal{K}_\mathrm{NIU} \cup \mathcal{K}_{\mathrm{IU}_1}$ and $\mathcal{K}_r \leftarrow \mathcal{K}_r \setminus \mathcal{K}_s$
  Set $\mathcal{N}_s \leftarrow \mathcal{N}_s \cup \mathcal{N}_\mathrm{NIU} \cup \mathcal{N}_{\mathrm{IU}_1}$ and $\mathcal{N}_r \leftarrow \mathcal{N}_r \setminus \mathcal{N}_s$
  Set $\mathbf{T} \leftarrow \left[\mathbf{T}(i,j)\right]_{i\in\mathcal{K}_r, j\in\mathcal{N}_r}$
end while
Constitute $\tilde{\mathbf{H}}_b = \left[\hat{\mathbf{H}}_b(:,n)\right]_{n\in\mathcal{N}_s}$

according to their channel norm in descending order. The user that has the highest channel norm is added to the set of selected users $\mathcal{U}$, first. Then, the algorithm selects the next user having the second-highest channel norm if the correlation between that user and the first one is less than ϵ. At each iteration, the candidate user is handled, and the correlation matrix $\mathbf{C}_b$ is computed over

$$\mathrm{c}_b(i,j) = \frac{|\hat{\mathbf{H}}_b(i,:)\hat{\mathbf{H}}_b(j,:)^H|}{\|\hat{\mathbf{H}}_b(i,:)\|\|\hat{\mathbf{H}}_b(j,:)\|}, \tag{15}$$

where the beamspace channel matrix of the selected users is $\hat{\mathbf{H}}_b = \left[\bar{\mathbf{H}}_b(s,:)\right]_{s\in\mathcal{U}}$. The algorithm continues until the number of elements in the set $\mathcal{U}$ is equal to K_u.

The second part of the proposed algorithm is the beam selection. Let define the set of remaining users, remaining beams, selected users, and selected beams as $\mathcal{K}_r$, $\mathcal{N}_r$, $\mathcal{K}_s$, and $\mathcal{N}_s$, respectively. Initially, the set of selected users and beams have no elements, and the set of remaining users and beams have all users that are selected before, and all beams. The algorithm searches the beams iteratively. In each iteration, the strongest or dominant beams for the remaining users are found out, ξ_k for $k \in \mathcal{K}_r$. If a beam is the strongest beam of more than one user, the algorithm adds those users to the set of interfering users, $\mathcal{K}_\mathrm{IU}$. But, if a beam is the strongest beam for only one user, that user is added to the set of non-interfering users, $\mathcal{K}_\mathrm{NIU}$, and the corresponding beam is added to the set of non-interfering users' beams, $\mathcal{N}_\mathrm{NIU}$. The algorithm assigns their strongest beams to the non-interfering users. For the interfering users, the set $\mathcal{K}_\mathrm{IU}$ is divided into subsets. The subset $\mathcal{A}_{\xi_m}^{(l)}$ contains the users sharing the same strongest beam ξ_m, and there are L subsets of $\mathcal{K}_\mathrm{IU}$. In each subset, the user that has the highest channel gain is investigated to assign the mentioned beam. Those users are added to the set $\mathcal{N}_{\mathrm{IU}_1}$. Then, the allocated users and beams are ejected from $\mathcal{K}_r$ and $\mathcal{N}_r$, respectively. For the remaining users, the algorithm follows the same steps until there is no user left.

The low dimensional system is formed by selecting a few number of beams such that

$$\tilde{\mathbf{H}}_b = \left[\hat{\mathbf{H}}_b(:,n)\right]_{n\in\mathcal{N}_s}, \tag{16}$$

where $\mathcal{N}_s$ is the set of selected beam indices. Then, the lower dimensional system representation is given as

$$\mathbf{r} = \tilde{\mathbf{H}}_b\tilde{\mathbf{W}}_b\mathbf{s} + \mathbf{n}, \tag{17}$$

where $\tilde{\mathbf{W}}_b \in \mathbb{C}^{K_u \times K_u}$ is the reduced dimensional precoder matrix which corresponds to $\tilde{\mathbf{H}}_b \in \mathbb{C}^{K_u \times K_u}$.

After the selection of K_u users and K_u beams is completed through **Algorithm 2**, the ZF precoding is performed as given in (8) using the $K_u \times K_u$ dimensional resulting channel matrix of $\tilde{\mathbf{H}}_b$.

IV. COMPLEXITY ANALYSIS

In this section, the computational complexity analyses of the proposed user selection methods are given to deduce their

computational efficiency against the benchmark methods. For the digital transceiver, an exhaustive search (ES) method can find the optimal solution for the sum data rate. Since it requires to search all possible K_u-element subsets of users over all K users, the computational complexity of ES in the digital scheme is given by $\mathcal{O}(K^{K_u})$. As a result, it leads to an exponentially growing complexity depending on the total number of users and the number of selected users [11]. On the other hand, Algorithm 1 finds a sub-optimal solution by eliminating the users based on the correlation. This method requires the computation of correlation matrix $\mathbf{C}$ at each iteration, and the dimension of the matrix changes with respect to the iteration. Therefore, the complexity of Algorithm 1 is $\mathcal{O}(N_{\mathrm{T}}K^3)$.

For the hybrid transceiver, the joint user and beam selection schemes offer complicated frameworks which evaluate the user-beam pairs from the set of all users and the set of all beams, jointly. For example, the ES for joint user and beam selection searches all user-beam combinations to maximize the sum data rate. Therefore, the complexity of the ES in the hybrid scheme is determined by $\mathcal{O}\left(\sum_{Q=1}^{N_{\mathrm{RF}}} \binom{K}{Q}\binom{N_{\mathrm{T}}}{Q}Q!\right)$. On the other hand, the Greedy based JBUS algorithm in [23] finds all beam combinations and searches the users which maximize the sum data rate for each beam combination. Thus, Greedy based JBUS offers a sub-optimal scheme with the complexity $\mathcal{O}\left(\sum_{Q=1}^{N_{\mathrm{RF}}} K\binom{N_{\mathrm{T}}}{Q}Q\right)$.

Conversely, Algorithm 2 applies the user selection and the beam selection sequentially, not jointly. Therefore, the complexity of the user and the beam selection parts are evaluated separately. In the user selection part, the algorithm computes the beamspace channel norms of all users and the correlation matrix by adding a new user at each iteration. Most of the complexity is calculated through the computation of the correlation matrix. Thus, the complexity of the user selection part in Algorithm 2 is $\mathcal{O}(N_{\mathrm{T}}K_u^3)$. In the beam selection part, the algorithm finds the beams that are allocated to the selected users, which are less than K. However, the number of iterations (line 24) is not definite, unlike the user selection part. If the total number of iterations is denoted by N_{iter}, the complexity of the beam selection part can be given as $\mathcal{O}\left(\sum_{q=1}^{N_{iter}}\left\{Card\left(\mathcal{K}_r^q\right).Card\left(\mathcal{N}_r^q\right)+\sum_{l=1}^{L} Card\left(\mathcal{A}_{\xi_m}^{q,l}\right)\right\}\right)$ where $\mathcal{K}_r^q$, $\mathcal{N}_r^q$, and $\mathcal{A}_{\xi_m}^{q,l}$ are the set of remaining users, the set of remaining beams, and the l^{th} subset of the set of interfering users at the q^{th} iteration, respectively. The number of iterations strongly affects the complexity of the beam selection. It depends on the beamspace channel, the number of selected users, and the user selection scheme. We will give the numerical results in terms of the number of iterations in the next section. We infer that the highly correlated users generally share the same strongest beam in the proposed beam selection. Since we eliminate the highly correlated users in the user selection part, we not only improve the sum data rate performance of the system but also reduce the number of iterations in the beam selection part. Therefore, the computational complexity in the beam selection part is reduced significantly by the proposed user selection.

TABLE 1. Simulation parameters.

Parameter	Value
Carrier frequency, f_c	28 GHz
Number of paths, N_p	2
d_e, d_a	$\lambda/2$
Elevation angular spread, δ_e	6 degrees
Azimuth angular spread, δ_a	180 degrees
Channel gain for LoS, $\beta_k^{(0)}$	$\mathbb{C}\mathcal{N}(0,1)$
Channel gain for NLoS, $\beta_k^{(p)}$	$\mathbb{C}\mathcal{N}(0,0.1)$
A-AoD for LoS, $\vartheta_k^{(0)}$	$\mathcal{U}(-\pi/2,\pi/2)$
E-AoD for LoS, $\varphi_k^{(0)}$	$\mathcal{U}(-\pi/2,\pi/2)$
A-AoD for NLoS, $\vartheta_k^{(p)}$	$\mathcal{U}(\vartheta_k^{(0)}-\delta_a/2\ ,\ \vartheta_k^{(0)}+\delta_a/2)$
E-AoD for NLoS, $\varphi_k^{(p)}$	$\mathcal{U}(\varphi_k^{(0)}-\delta_e/2\ ,\ \varphi_k^{(0)}+\delta_e/2)$

V. SIMULATION RESULTS

In this section, we evaluate the sum data rate performance of NURA based FD-MIMO mmWave systems for both digital and hybrid transceivers in both sparse and dense scenarios. The performance evaluations are provided for the digital and the hybrid transceivers based on the simulation parameters given in Table 1 [7], [17], [25].

Firstly, the performance of the FD-MIMO with NURA in the digital transceivers is evaluated for the sparse scenarios where the number of users is less than or equal to the number of RF chains to provide the optimal NURA designs. Then, the performance of the user selection algorithm in the FD-MIMO with NURA using the digital transceivers is provided for the dense scenarios where the number of users is much higher than the number of RF chains. Finally, considering hybrid transceivers, the performance of the proposed user and beam selection algorithm in the FD-MIMO with NURA is obtained for the dense scenarios.

A. DIGITAL TRANSCEIVER IN SPARSE ENVIRONMENT

For the sparse environment which has $K \leq N_{\mathrm{RF}} = N_{\mathrm{T}}$, the performances of URA and NURA configurations with the same number of antennas in the azimuth and the elevation domains are evaluated. Also, the sum data rate performances of rectangular array configurations depending on the exponent η are investigated to conclude the optimal NURA design for a specific antenna dimension.

To that end, Fig. 3 illustrates the performance of 4×4 array antenna with respect to the exponent η when the number of users $K = K_u = 8, 10, 12$. The results indicate that the data rates per user of the NURA configurations with the exponent $0.15 \leq \eta \leq 2$ for $K = 8$, $0.20 \leq \eta \leq 2$ for $K = 10$ and $0.25 \leq \eta \leq 2$ for $K = 12$ are greater than their URA counterpart whose exponents are $\eta = 1$ for all

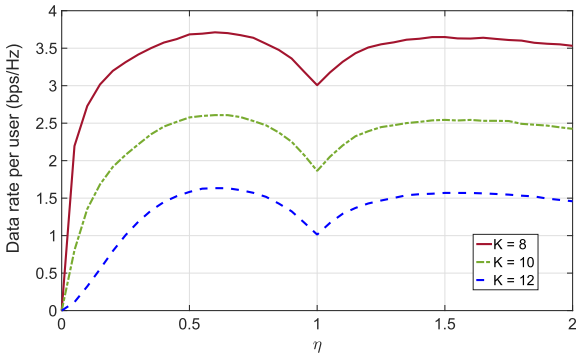

FIGURE 3. Data rate per user versus η for 4×4 array at $\rho = 30$dB for $K = K_u = 8, 10, 12$.

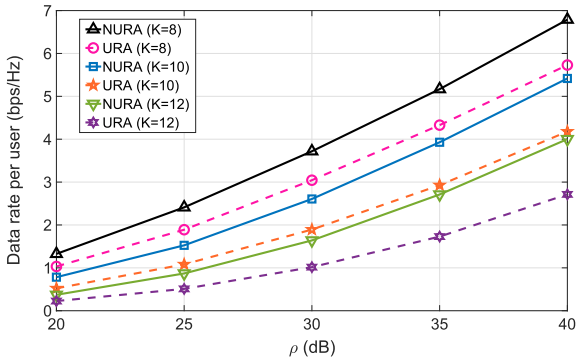

FIGURE 4. Data rate per user results of 4×4 URA and NURA for $\eta = 0.65$ and $K = K_u = 8, 10, 12$.

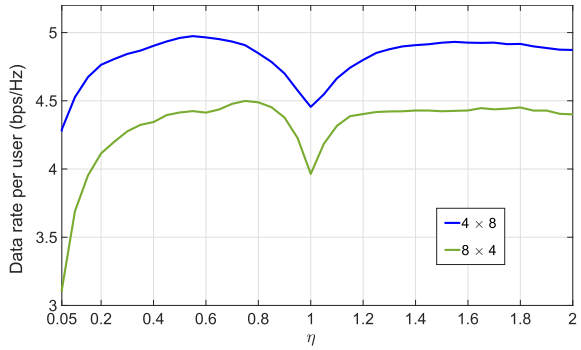

FIGURE 5. Data rate per user versus η for 4×8 and 8×4 arrays at $\rho = 30$dB for $K = K_u = 8$.

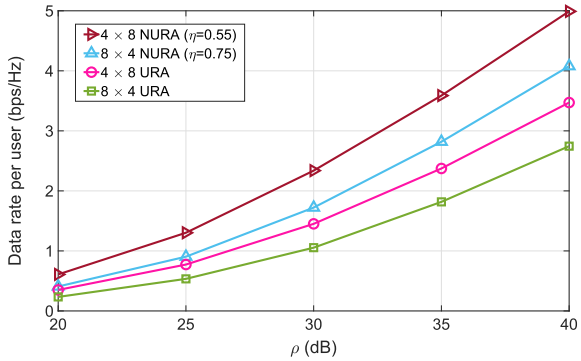

FIGURE 6. Data rate per user results of 4×8 and 8×4 arrays for $K = K_u = 16$.

K values. It is remarkable that for the different number of users, the optimal η value is approximately 0.65. Supporting nearly stable η value is a significant property of optimized NURA. Therefore, optimized 4×4 NURA configuration is practicable regardless of the number of users.

In Fig. 4, the performance evaluation is provided for 4×4 URA and NURA with the different number of users and 16 RF chains. As the number of users K is increased, meaning that the correlations between the users' channels are getting higher, the data rate per user for both URA and NURA decreases. On the other hand, the data rate difference between URA and NURA enhances as K_u is increased.

Fig. 5 depicts the data rate per user versus η for 4×8 and 8×4 arrays for $K = K_u = 8$. The optimum exponent is nearly 0.55 for 4×8 NURA whereas it is about 0.75 for 8×4 NURA structure. For the remaining part of the simulation results, these optimized exponent values for different antenna structures are kept.

Fig. 6 illustrates the data rate comparison of the systems with 4×8 and 8×4 array antennas. These systems utilizing digital beamformers have an equal number of RF chains and an equal number of users. Also, their optimized η values obtained from Fig. 5 are used. The data rate results demonstrate that the optimized 4×8 NURA configuration provides the best performance. When the number of antennas in the elevation domain is greater than that in the azimuth domain, the performance is degraded since the correlation between the users is increased.

B. DIGITAL TRANSCEIVER IN DENSE ENVIRONMENT

In the dense environment, the performance of the proposed user selection algorithm is compared with the user selection based on the channel norm which selects K_u users having the highest channel gains.

Fig. 7 demonstrates the sum data rate performance for different ρ values when the system contains 4×4 array and $K = 24$ users by selecting $K_u = 16$ users which is equal to the number of RF chains. The proposed algorithm with NURA provides a 22 bps/Hz higher sum data rate at $\rho = 40$dB compared to the channel norm based user selection with NURA. Besides, compared to the URA case, the proposed algorithm with NURA improves the sum data rate performance with a percentage of 20%.

Fig. 8 provides the sum data rate results for the proposed algorithm with different NURA structures when $K = 48$. The proposed algorithm selects $K_u = 8$ users for all cases. A higher number of antennas employed at the BS supports greater multiple antenna gain through a higher number of RF chains. Therefore, 4×8 and 8×4 NURA structures provide higher sum data rates. On the other hand, the correlation between the user channels is much higher when the number of antennas in the elevation domain is greater than that in the azimuth domain. As a result of that, 4×8 NURA provides better performance than 8×4 in the NURA structures.

Fig. 9 shows the sum data rate with respect to K when K_u is fixed. The higher number of users in the system, which

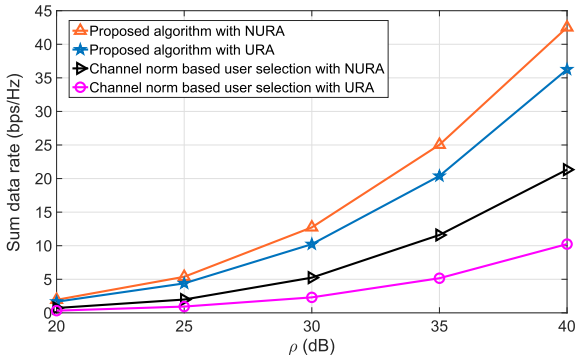

FIGURE 7. Sum data rate comparison of user selection schemes for 4 × 4 URA and NURA, $K = 24$ and $K_u = 16$.

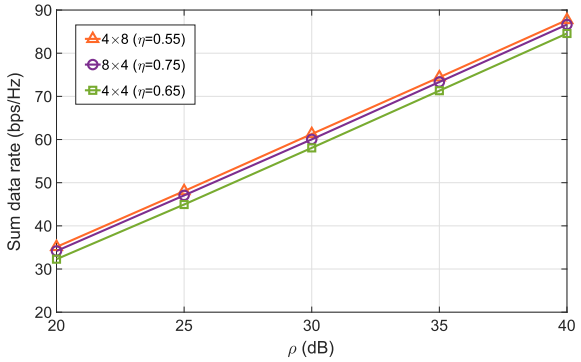

FIGURE 8. Sum data rate results of the proposed user selection algorithm with different NURA structures, $K = 48$, $K_u = 8$.

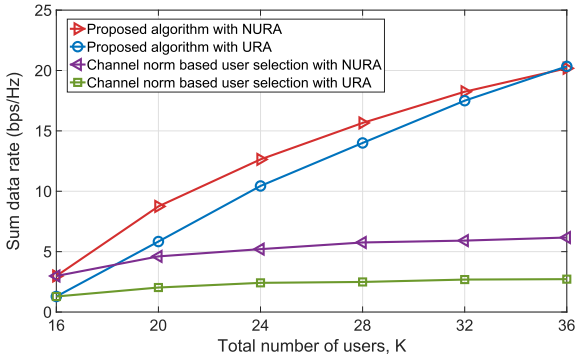

FIGURE 9. Sum data rate comparison versus K for 4 × 4 NURA and URA, $K_u = 16$ and $\rho = 30$dB.

corresponds to the dense environment, provides better elimination of highly correlated users with the proposed algorithm. Therefore, the sum data rate performance of the proposed user selection is increased.

C. HYBRID TRANSCEIVER IN DENSE ENVIRONMENT

In the dense environment, the performance of the proposed user and beam selection algorithm is compared with the channel norm based user selection combined with the proposed beam selection in Algorithm 2 - Part 2, and the joint user and beam selection algorithm in [23]. Also, the effect of the threshold value on the sum data rate of the system is

TABLE 2. Parameters of the simulation environments.

Parameter	Environment 1	Environment 2	Environment 3
N_{T}	4×8	8×4	8×8
K	24	24	48
N_{RF}	16	16	32

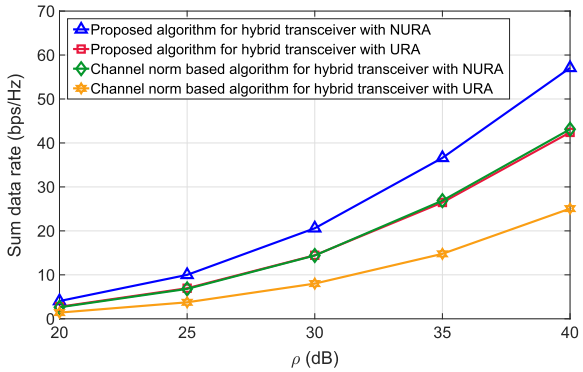

FIGURE 10. Sum data rate comparison of user selection schemes for the environment 1 and $\epsilon = 0.9$ in the hybrid transceiver.

investigated. In the performance evaluations, N_{RF} is determined as half of N_{T}, and K is one and half of N_{RF}. Moreover, a large number of antennas can be utilized in the hybrid transceiver from the point of power efficiency and hardware complexity. Thus, the performance results of 8×8 antenna configurations are provided in this section. Table 2 describes the simulation environments used in the following performance evaluations.

Fig. 10 provides the sum data rate comparison of the proposed user and beam selection algorithm with $\epsilon = 0.9$ and the channel norm based algorithm in the environment 1. It illustrates that the proposed user and beam selection algorithm with NURA configuration provides approximately 43% higher sum data rate compared to the channel norm based algorithm. Also, the proposed user and beam selection algorithm utilizing NURA achieves significant gain compared to the same scheme utilizing URA structure.

Fig. 11 and Fig. 12 illustrate the performance comparisons of the proposed algorithm for the environment 2 and 3, respectively when the threshold value is determined as 0.9. In environment 2, the proposed algorithm with NURA achieves the sum data rate nearly two times of the sum data rate achieved by the channel norm based algorithm with NURA. Besides, the proposed algorithm with NURA outperforms its URA counterpart by 5%. In environment 3, the proposed user and beam selection algorithm provides the sum data rate by more than 2.5 times of the channel norm based algorithm through NURA configuration.

Fig. 13 provides the sum data rate of the proposed algorithm with respect to the number of users for 4×8 and 8×4. It is shown that selecting N_{RF} users from a large number of users gives more degree of freedom. Therefore, the sum data rate improves when the number of users is

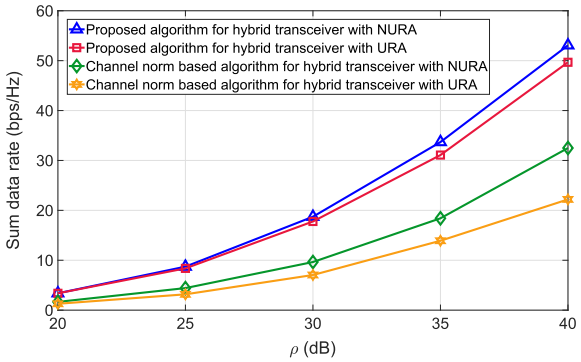

FIGURE 11. Sum data rate comparison of user selection schemes for the environment 2 and $\epsilon = 0.9$ in the hybrid transceiver.

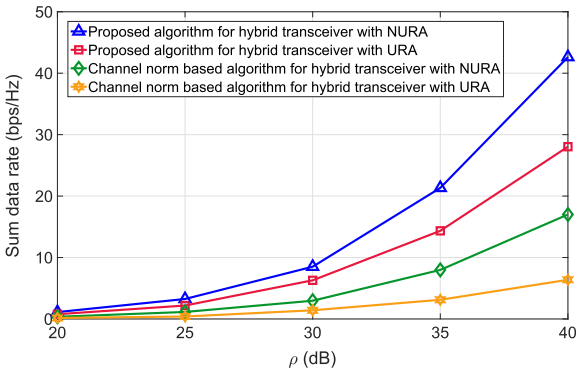

FIGURE 12. Sum data rate comparison of user selection schemes for the environment 3 and $\epsilon = 0.9$ in the hybrid transceiver.

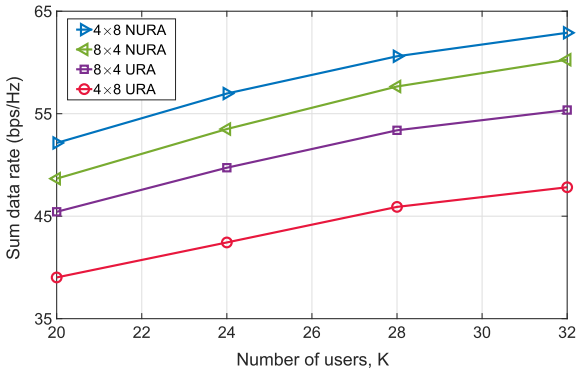

FIGURE 13. Sum data rate versus K for 4×8 and 8×4 arrays, $K_u = N_{RF} = 16$ in the hybrid transceiver at $\rho = 40$dB.

increased whereas the proposed algorithm for 4×8 NURA configuration provides the best performance.

To reveal the feasibility of the proposed user and beam selection, the comparison result with the Greedy based JBUS algorithm in [23] is provided as the benchmark method for the beamspace mmWave MIMO system. In Fig. 14, the sum data rate comparison of the proposed user and beam selection algorithm and the Greedy based JBUS for the optimized 4×8 NURA configuration is shown. Due to the excessive computational complexity of the Greedy based JBUS algorithm, it is only demonstrated the sum data rate results when the number of RF chains is relatively small such as $N_{RF} = 4$

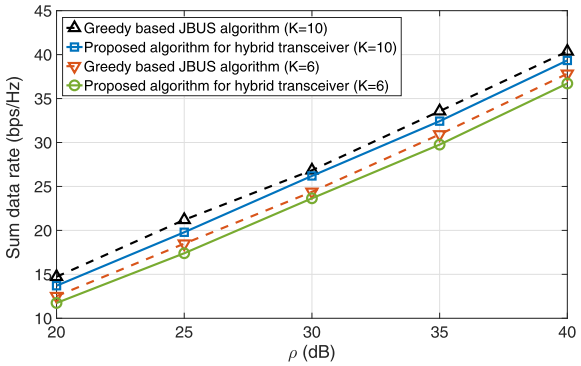

FIGURE 14. Sum data rate comparison of the proposed algorithm and the Greedy based JBUS for 4×8 NURA, $K_u = N_{RF} = 4$, and $\epsilon = 0.9$ in the hybrid transceiver.

considering the different number of users. It is shown that the Greedy based JBUS can solely provide 4.6% higher sum data rate than the proposed user and beam selection for both $K = 6$ and $K = 10$ although its huge complexity. On the other hand, the proposed one completes its beam selection part in $N_{iter} = 1.3$ iterations on average.

VI. CONCLUSION

In this work, the user and beam selection has been investigated in the mmWave non-uniform FD-MIMO systems utilizing both fully digital and hybrid analog/digital transceivers. For the digital transceiver, we have proposed the decremental user selection algorithm enabling to serve the users through mmWave non-uniform FD-MIMO in the dense environment. The performance results have verified that the correlation between the users' channels degrades the performance. The proposed user selection based on the correlation has achieved better performance on the sum data rate. Furthermore, the optimal NURA configuration has been investigated, and it has been demonstrated that the optimized NURA outperforms its URA counterpart. Besides, we have proposed the sequential user and beam selection algorithm handling the non-uniform FD-MIMO with the beamspace MIMO concept in the hybrid transceiver. The beam selection by exploiting the sparsity inherent in the beamspace channel has been applied along with the user selection. The performance evaluations have illustrated the gain of the proposed algorithm with optimized threshold values on the sum data rate under non-uniform FD-MIMO with hybrid architectures. Moreover, the feasibility of the proposed algorithm has been demonstrated through its achievable sum data rate while requiring much lower computational complexity compared to the joint user and beam selection scheme.

REFERENCES

[1] V. W. Wong, R. Schober, D. W. K. Ng, and L.-C. Wang, *Key Technologies for 5G Wireless Systems*. Cambridge U.K.: Cambridge Univ. Press, 2017.

[2] M. Xiao, S. Mumtaz, Y. Huang, L. Dai, Y. Li, M. Matthaiou, G. K. Karagiannidis, E. Björnson, K. Yang, C.-L. I, and A. Ghosh, "Millimeter wave communications for future mobile networks," *IEEE J. Sel. Areas Commun.*, vol. 35, no. 9, pp. 1909–1935, Sep. 2017.

[3] K. Zrar Ghafoor, L. Kong, S. Zeadally, A. S. Sadiq, G. Epiphaniou, M. Hammoudeh, A. K. Bashir, and S. Mumtaz, "Millimeter-wave communication for Internet of Vehicles: Status, challenges, and perspectives," *IEEE Internet Things J.*, vol. 7, no. 9, pp. 8525–8546, Sep. 2020.

[4] Y.-H. Nam, B. Ng, K. Sayana, Y. Li, J. Zhang, Y. Kim, and J. Lee, "Full-dimension MIMO (FD-MIMO) for next generation cellular technology," *IEEE Commun. Mag.*, vol. 51, no. 6, pp. 172–179, Jun. 2013.

[5] X. Li, C. Li, S. Jin, and X. Gao, "Fair downlink transmission for multi-cell FD-MIMO system exploiting statistical CSI," *IEEE Commun. Lett.*, vol. 22, no. 4, pp. 860–863, Apr. 2018.

[6] W. Liu, Z. Wang, C. Sun, S. Chen, and L. Hanzo, "Structured non-uniformly spaced rectangular antenna array design for FD-MIMO systems," *IEEE Trans. Wireless Commun.*, vol. 16, no. 5, pp. 3252–3266, May 2017.

[7] W. Liu and Z. Wang, "Non-uniform full-dimension MIMO: New topologies and opportunities," *IEEE Wireless Commun.*, vol. 26, no. 2, pp. 124–132, Apr. 2019.

[8] Y. Tsai, L. Zheng, and X. Wang, "Millimeter-wave beamformed full-dimensional MIMO channel estimation based on atomic norm minimization," *IEEE Trans. Commun.*, vol. 66, no. 12, pp. 6150–6163, Dec. 2018.

[9] J. Mao, J. Gao, Y. Liu, and G. Xie, "Simplified semi-orthogonal user selection for MU-MIMO systems with ZFBF," *IEEE Wireless Commun. Lett.*, vol. 1, no. 1, pp. 42–45, Feb. 2012.

[10] R. Rajashekar and L. Hanzo, "User selection algorithms for block diagonalization aided multiuser downlink mm-Wave communication," *IEEE Access*, vol. 5, pp. 5760–5772, 2017.

[11] K. Aldubaikhy, W. Wu, Q. Ye, and X. Shen, "Low-complexity user selection algorithms for multiuser transmissions in mmWave WLANs," *IEEE Trans. Wireless Commun.*, vol. 19, no. 4, pp. 2397–2410, Apr. 2020.

[12] J. Choi, G. Lee, and B. L. Evans, "User scheduling for millimeter wave hybrid beamforming systems with low-resolution ADCs," *IEEE Trans. Wireless Commun.*, vol. 18, no. 4, pp. 2401–2414, Apr. 2019.

[13] S. Jun, D. Kim, and J. Kang, "User selection for multi-user mmWave systems with phased-zero-forcing hybrid precoder," in *Proc. 14th IEEE Annu. Consum. Commun. Netw. Conf. (CCNC)*, Las Vegas, NV, USA, Jan. 2017, pp. 684–686.

[14] H. Wu, D. Liu, W. Wu, C. Na, and M. Liu, "A low complexity two-stage user scheduling scheme for mmWave massive MIMO hybrid beamforming systems," in *Proc. 3rd IEEE Int. Conf. Comput. Commun. (ICCC)*, Chengdu, China, Dec. 2017, pp. 945–951.

[15] A. Sayeed and J. Brady, "Beamspace MIMO for high-dimensional multiuser communication at millimeter-wave frequencies," in *Proc. IEEE Global Commun. Conf. (GLOBECOM)*, Dec. 2013, pp. 3679–3684.

[16] P. V. Amadori and C. Masouros, "Low RF-complexity millimeter-wave beamspace-MIMO systems by beam selection," *IEEE Trans. Commun.*, vol. 63, no. 6, pp. 2212–2223, Jun. 2015.

[17] X. Gao, L. Dai, Z. Chen, Z. Wang, and Z. Zhang, "Near-optimal beam selection for beamspace mmWave massive MIMO systems," *IEEE Commun. Lett.*, vol. 20, no. 5, pp. 1054–1057, May 2016.

[18] R. Pal, A. K. Chaitanya, and K. V. Srinivas, "Low-complexity beam selection algorithms for millimeter wave beamspace MIMO systems," *IEEE Commun. Lett.*, vol. 23, no. 4, pp. 768–771, Apr. 2019.

[19] S. He, Y. Wu, D. W. K. Ng, and Y. Huang, "Joint optimization of analog beam and user scheduling for millimeter wave communications," *IEEE Commun. Lett.*, vol. 21, no. 12, pp. 2638–2641, Dec. 2017.

[20] H. Xu, J. Yu, and S. Zhu, "Ping-pong optimization of user selection and beam allocation for millimeter wave communications," *IEEE Access*, vol. 7, pp. 133178–133189, 2019.

[21] H. Xu, S. Zhu, and P. Cui, "Joint optimization of beam selection and user scheduling for mmWave massive MIMO communication system," in *Proc. IEEE 19th Int. Conf. Commun. Technol. (ICCT)*, Oct. 2019, pp. 653–657.

[22] Z. Jiang, S. Chen, S. Zhou, and Z. Niu, "Joint user scheduling and beam selection optimization for beam-based massive MIMO downlinks," *IEEE Trans. Wireless Commun.*, vol. 17, no. 4, pp. 2190–2204, Apr. 2018.

[23] Z. Cheng, Z. Wei, and H. Yang, "Low-complexity joint user and beam selection for beamspace mmWave MIMO systems," *IEEE Commun. Lett.*, vol. 24, no. 9, pp. 2065–2069, Sep. 2020.

[24] Y. Yang, S. Dang, M. Wen, S. Mumtaz, and M. Guizani, "Mobile millimeter wave channel tracking: A Bayesian beamforming framework against DOA uncertainty," in *Proc. IEEE Global Commun. Conf. (GLOBECOM)*, Dec. 2019, pp. 1–6.

[25] X. Li, S. Jin, H. A. Suraweera, and X. Gao, "Line-of-sight based statistical 3D beamforming for downlink massive MIMO systems," in *Proc. IEEE Int. Conf. Commun. (ICC)*, May 2016, pp. 1–6.

[26] J. Brady, N. Behdad, and A. M. Sayeed, "Beamspace MIMO for millimeter-wave communications: System architecture, modeling, analysis, and measurements," *IEEE Trans. Antennas Propag.*, vol. 61, no. 7, pp. 3814–3827, Jul. 2013.

[27] J. Brady and A. Sayeed, "Beamspace MU-MIMO for high-density gigabit small cell access at millimeter-wave frequencies," in *Proc. IEEE 15th Int. Workshop Signal Process. Adv. Wireless Commun. (SPAWC)*, Jun. 2014, pp. 80–84.